Title
THE DYNAMICS OF VISCOUS NUCLEAR DROPS

Author
Alonso, Carol Travis.

Publication Date
1974-08-01

Presented in part at the International
Colloquium on Drops and Bubbles,
Pasadena, CA, August 28-30, 1974

THE DYNAMICS OF VISCOUS NUCLEAR DROPS

Carol Travis Alonso

August 1974

Prepared for the U.S. Atomic Energy Commission
under Contract W-7405-ENG-48

DISCLAIMER

LBL-2993

THE DYNAMICS OF VISCOUS NUCLEAR DROPS

Carol Travis Alonso

Lawrence Berkeley Laboratory
University of California
Berkeley, California 94720

August 1974

CONTENTS

ABSTRACT

I. INTRODUCTION

II. THE NUCLEAR FLUID

A. Nuclear Rheology

B. Nuclear Hydrodynamics

III. HYDRODYNAMIC THEORY

A. Bulk Equations

B. Boundary Conditions at the Free Surface

C. The Computer Code "SQUISH"

IV. SIMULATIONS OF DROP DYNAMICS

A. Oscillations

B. Fissions

C. Fusions

V. SUMMARY

ACKNOWLEDGMENTS

REFERENCES

LBL-2993

THE DYNAMICS OF VISCOUS NUCLEAR DROPS *†

Carol Travis Alonso

Lawrence Berkeley Laboratory
University of California
Berkeley, California 94720

ABSTRACT

We present here a dynamical description of the oscillation, fission, and fusion of classical viscous charged or gravitating liquid drops. This description is generated numerically by computer simulation. While the emphasis is on drops scaled to nuclear dimensions, the application is general. The methods described here will be applied to problems in astrophysics, meteorology, fluid mechanics, and space science. This paper is intended as a preliminary survey of drop dynamics; subsequent papers will study each class of motion more thoroughly.

We include here a discussion of the applicability of the classical hydrodynamic approach to the nuclear problem. This is followed by a description of the bulk flow equations and free surface boundary conditions for a viscous charged drop. Finally we present some simulations of the oscillations of charged and neutral drops as a function of initial shape, charge, and viscosity. We also present some preliminary simulations of fissions and fusions of viscous charged drops, with some comments about the possible role of nuclear viscosity in the creation of "superheavy" elements in heavy ion accelerator experiments.

* Presented in part at the International Colloquium on Drops and Bubbles, Pasadena, California, August 28-30, 1974.

† Prepared under the auspices of the United States Atomic Energy Commission.

I. INTRODUCTION

We present in this paper a dynamical description of the oscillation, fission, and fusion of classical liquid drops. This description is generated numerically by computer simulation. While the emphasis is on drops scaled to nuclear dimensions, the application is general by virtue of dynamic similarity. Since this paper is directed toward non-nuclear as well as nuclear scientists, we have attempted to relate some nuclear aspects to more common fluid flow phenomena. The methods described here will be applied to problems in astrophysics, meteorology, fluid mechanics, and even space science. The results presented in this paper represent only a preliminary survey of drop dynamics; subsequent papers will study each class of motion separately and thoroughly.

The general problem of liquid drop dynamics, important as it is to many scientific investigations, has never been fully solved due to the complexity of the hydrodynamic equations involved. Small amplitude oscillations have been treated analytically by Rayleigh[1], Chandrasekhar[2], and others[3,4]. Large-amplitude oscillations and distortions, including the fission and fusion of liquid drops, cannot be described analytically in complete detail.

In the particular field of nuclear hydrodynamics, it has become of critical importance to be able to follow in some way the dynamic path of those large amplitude motions leading to nuclear fusion and fission. Some studies of this problem using parameterized surfaces and irrotational flow have been carried out by Sierk and Nix[5]. Other efforts have concentrated on solutions of Hamilton's equations using parameterized shapes[6]. Disruptive processes such as fusion have not been studied dynamically because they do not lend themselves easily to shape parameterization. The question of nuclear viscosity, which can transfer collective energy to single-particle excitations, is also relatively unexplored in nuclear dynamics.

In order to study these large-amplitude processes we are developing a hydrodynamic computer code which simulates them for viscous incompressible drops endowed with a body charge and surface tension. The corresponding application to gravitating drops is straightforward. Our code traces the dynamic evolution of an axially-symmetric system as a function of time. It utilizes a free surface that requires no parameterization, and its velocity field can be rotational or irrotational as required. The present version calculates the relevant energies, velocity fields, moments and shapes as a function of viscosity, time, and such initial conditions as charge, surface tension, energy, and shape.

We present here some studies of the oscillations of charged and neutral drops as a function of initial shape, charge, and viscosity. We also present some preliminary simulations of fissions and fusions of viscous charged drops, with some comments about the possible role of nuclear viscosity in the creation of "superheavy" elements in heavy ion accelerator reactions.

In the first section we present some arguments and speculations concerning the applicability of the classical macroscopic approach to nuclear problems. Parts of this section have been included for the benefit of the non-nuclear

scientist, and other parts are more familiar to researchers outside of nuclear physics. The subsequent section describes the computer code, and then the final section discusses some of the results that have been obtained with this code.

II. THE NUCLEAR FLUID

During the last three decades an enormous amount of experimental data has accumulated in studies of nuclear fission. The more recent advent of high-resolution detectors has resulted in a rather complete study of nuclear vibrations and rotations. In this decade, the new heavy ion accelerators have begun to provide data on the properties of nuclear fusion. These three dynamical processes of nuclear fission, oscillation, and fusion all display, under certain conditions, a collective motion in which individual nucleons are capable of moving together in a coherent flow pattern that is similar to classic fluid flow.

The non-nuclear scientist, remembering the quantum mechanical description of widely separated individual nuclear states, wonders under what conditions the nucleus behaves like a classical liquid. In this section we shall describe those conditions and discuss the nature of the nuclear fluid.

A. Nuclear Rheology

Atomic nuclei are "glued" together, despite their repulsive body charge, by strong attractive short-range nuclear forces. These forces resemble the cohesive Van der Waals forces between molecules. Some time ago Brueckner[7] made some detailed calculations of the bulk properties of infinite uniform nuclear matter. These calculations were microscopic; that is, he assumed a momentum-dependent potential in the Schroedinger equation and calculated the motions of individual nucleons. The physical consequence of this form of potential is that the positions of neighboring nucleons are correlated. In the neighborhood of a particle center there may be density fluctuations, but the distribution of these fluctuations is uniform and continuous.

This picture of particles forming fluctuating clusters with their nearest neighbors corresponds to the current theory of the liquid state[8]. In Figure 1-a is shown a simplified comparison of the microscopic clustering observed in solids, liquids, and gases. The radial distribution function f_r measures the probability of encountering another particle at a distance r from a particle center. Gas particles move in a uniform and uncorrelated manner. Solid particles are correlated in a periodic lattice. Particles in a liquid lie between these two extremes, with a strong correlation only in the vicinity of the particle center.

We wish to explore under what conditions nuclear matter should be treated as a solid or a liquid or a gas. These conditions depend mainly on how the time scale of a dynamic process compares with the relaxation time for nearest-neighbor correlations. In Figure 1-b are shown schematic representations of how nearest-neighbor correlations relax as a function of time after an initial impulse is delivered to an individual particle. For ideal gases there is no correlation after the impulse, but as the material becomes more and more rigid the relaxation time gets longer and longer. To calculate the relaxation time

for nuclear matter, we borrow some concepts from the science of rheology, which is concerned with combining the properties of solids and liquids to describe particular classes of materials. Some important classes include Kelvin bodies, Maxwell bodies, and Bingham bodies, each with a different stress equation. These major rheological types combine the effects of a Hookean elastic solid, for which

$$\sigma = \mu \gamma \tag{1}$$

(where σ is the stress, μ the modulus of rigidity, and γ the angular shear) and a Newtonian liquid, for which

$$\sigma = \eta \dot{\gamma} \tag{2}$$

(where η is the viscosity). Let us suppose that the nuclear material is a Maxwell body, with the rheological equation[9]

$$\dot{\gamma} = \frac{\dot{\sigma}}{\mu} + \frac{\sigma}{\eta} \quad . \tag{3}$$

This equation describes a viscoelastic material that is predominantly in the liquid state. This fits our experimental description of the nucleus as a material which behaves like a liquid in its fission dynamics and which can sustain permanent deformations. The solution to this differential equation, assuming $\dot{\gamma} = 0$, is

$$\sigma = \dot{\gamma}\eta + (\sigma_o - \dot{\gamma}\eta) \, e^{-t/\lambda} \tag{4}$$

where $\lambda = \eta/\mu$ is the relaxation time for the stress. If a dynamic process takes place in a time $\tau >> \lambda$ the material behaves like a fluid, but if $\tau << \lambda$ it behaves like a solid. Typical relaxation times for various common materials are quoted by Reiner[9] to be of the order of:

10^{-9} sec for air

10^{2} sec for pitch

10^{7} sec for glass .

An estimate of λ for nuclear matter is difficult because we know neither the viscosity η nor the modulus of rigidity μ. This latter quantity can be roughly estimated from the nuclear spring constant κ = 1-10 Mev/fm^2 that is fitted to the minimum of a liquid drop potential[10]. Assuming the simple relationship

$$\mu = \frac{\text{stress}}{\text{strain}} = \frac{\kappa \Delta R/\pi R^2}{\Delta R/R} = \kappa/\pi R \tag{5}$$

we estimate that $\mu \sim 0.1$ MeV/fm^3. (See Table I for Nuclear Units)

In order to estimate λ we must also assign a value to the viscosity η. The nuclear viscosity is probably highly temperature dependent. The viscosity of the well known Fermi-liquid ^{3}He displays the temperature dependence[11] shown on the left of Figure 2, and we might speculate that nuclear matter has a temperature dependence such as that shown on the right. At low temperatures the nuclear fluid has strong pairing correlations that could lead to superfluid flow, but at higher temperatures it may approach the T^{-2} law of normal Fermi liquids. At classical temperatures the viscosity of an ideal gas goes as $T^{\frac{1}{2}}$ and is independent of the density. Thus spontaneous nuclear fission, a low-temperature phenomenon, may show no viscous effects, while accelerator-induced fusion and fission, which usually take place at higher temperatures, may display substantial viscous effects. The recent failures to produce superheavy elements by heavy ion fusion reactions[12] could be attributed to a high nuclear viscosity. The effect of this viscosity would be to convert the energy of the forward motion of the fusion process into frictional heating, making fusion impossible due to the repulsive Coulomb forces that always tend to pull distorted shapes apart. In view of the fact that low-temperature nuclear processes such as vibrations seem to be underdamped whereas higher-temperature nuclear processes may be overdamped, let us assume that the nuclear viscosity has the critical value for surface oscillations, which is around 0.5 MeV dsec/fm^3. This agrees with other recent estimates made by Sussman[13]. Using this value we find that the rheological relaxation time λ is of the order of 0.2 dsec.

A typical nucleon moves with a radius of several fm and a speed of about 8 fm/dsec. Thus a characteristic time for nucleon motion is of the order of one dsec. Direct reactions, in which a few nucleons are transferred from target to projectile, take place in about a few dsec. Spontaneous fission from saddle to scission requires about 50 dsec, and the fusion process can take up to 100 dsec. Comparing these times to our estimate of λ, we conclude that all of these processes, especially fission and fusion, require a fluid model for calculations of their dynamics. In the next sub-section we discuss what kinds of fluids are applicable for the different types of processes.

B. Nuclear Hydrodynamics

In certain cases the nuclear fluid can be treated either as a Fermi gas or a classical gas, depending on the temperature. The former case is true in fast reactions which involve only a few nucleons. For example, in the grazing collision of two heavy nuclei, where there is the direct transfer of one or two nucleons between target and projectile, a Fermi gas model is useful. Experimentally these nucleons are observed to drop into the quantum-mechanical energy shells of the target nucleus without disturbing the bulk of the nucleus. Another example is the relativistic head-on collision of two heavy nuclei, where a classical gas model is appropriate even though the bulk of the nucleus is involved. The basic criterion for a gas model is that during the dynamic process there is not enough time for the establishment of nearest-neighbor correlations.

In general a liquid model should be used for non-relativistic processes involving the interaction of many nucleons. For example the slow head-on fusion of two heavy nuclei involves hundreds of nucleons. During the collision, the disturbed nucleons share many quantum states with their neighbors, and the

shell structure is "smeared" out to resemble a liquid state continuum. This liquid can be quantum-mechanical or classical depending on the temperature. In Figure 3 we have attempted to show where the physics of heavy nuclei fits in the transition from the quantum-mechanical to the classical regimes. The transition point is taken to be at the temperature where the de Broglie wavelength equals the internucleon spacing:

$$\lambda\!\!\!^{-} = \frac{\hbar}{p} = \sqrt{\frac{\hbar^2}{2MkT_o}} = d = 2\text{fm} . \qquad (6)$$

For comparison, typical nuclear "temperatures" are of the order of 10^9°K (0.1 MeV). The transition temperature of ^{3}He is at 3°K (2×10^{-4} eV) and that of the metallic electron gas at 50,000°K (4 eV), so liquid ^{3}He would be classical at room temperature and the electron gas is very quantum-mechanical.

Figure 3 illustrates a basic problem in heavy ion dynamical calculations: the processes of most interest, especially fusion, lie in the transition region, where theoretical calculations are extremely difficult. For this reason we have traditionally attacked this problem from the quantum side or the classical side and then tried to treat one as a perturbation on the other.

It is interesting to make further comparisons of this unique nuclear fluid with the other two well known Fermi fluids mentioned above. The nuclear fluid in many ways lies between liquid ^{3}He and the electron gas in its properties. This is illustrated by the square in Figure 4, which places the three Fermi liquids qualitatively with respect to the strengths of the four quantities on the sides, namely density, state, Coulomb effects, and pairing effects. Proceeding clockwise around the square and starting at the bottom, we have observed that the pairing correlation in the electron gas is strong enough to make superconductors at low temperatures. Pairing effects are observed as medium-strength perturbations on nuclear states, and an extremely small pairing has only recently been observed in ^{3}He[14]. On the left side of the square are compared the ratios of density to close-packed density. Brueckner has pointed out that ρ/ρ_c is ten times larger for liquid ^{3}He than for nuclear matter[15]. (The nuclear density is around 0.1 nucleon/fm^3). The top of the square again reflects this density change. Finally, the right side of the square compares Coulomb effects. These are very different for the three fluids. ^{3}He is basically neutral, and charged Fermi liquids behave quite differently from neutral liquids because of the long range of the Coulomb forces. The metallic electron gas is not very much like a nucleus because its charge density is modulated by a background of the opposite charge which causes screening and dressing. The nucleus is the only volume-charged Fermi liquid available at low temperatures, and this may lead to the discovery of some exciting new bulk properties in the future.

A final consideration concerns the appropriateness of assuming a macroscopic approach to classical nuclear hydrodynamics. One criterion for the validity of the Navier-Stokes equation for fluid flow is that the period of the fluid motion be long compared to the characteristic nucleon time of 1 dsec. This criterion is met for such dynamic processes as fusion and fission. Another criterion is that

the mean free path of individual nucleons be small compared to a characteristic length of the fluid. For this we compare the average mean free path of 1.2 fm ($\ell = 1/n\sigma$; $n = .13$ nucleon/fm^3 and $\sigma = \pi a^2 \approx 6$ fm^2) with the nuclear radius, which ranges from 1 to 10 fm. This suggests that a macroscopic approach is valid only for the heaviest nuclei, and in particular this approach is not very applicable to "light" heavy ions such as oxygen or neon. Also flow problems involving thin constrictions will require microscopic adjustments.

In the spirit of this macroscopic classical assumption, we have developed a computer code called SQUISH that solves the problem of fluid flow for a system of incompressible drops with sharp surfaces. The incompressibility is a good approximation for heavy nuclear drops at ordinary accelerator temperatures and below. At higher excitation energies (for example, Bevalac energies), a compressible model should be used. The following section is a description of the computer code, and this is followed by some results for oscillations, fissions, and fusions.

III. HYDRODYNAMIC THEORY

A description of liquids with free surfaces requires a set of bulk equations for the general flow coupled with a set of free surface boundary conditions. In liquid drops the boundary conditions dominate the dynamics. In this section we discuss the bulk and surface equations and how they are handled by the computer code "SQUISH".

A. The Bulk Equations

Assuming a constant coefficient of viscosity, the two equations that govern viscous flow are the equation of continuity

$$\frac{\partial \rho}{\partial t} + \bar{\nabla} \cdot \rho \bar{u} = 0 \tag{7}$$

and the Navier-Stokes equation for Newtonian fluids

$$\left(\frac{\partial}{\partial t} + \bar{u} \cdot \bar{\nabla}\right) \bar{u} = \frac{-1}{\rho} \bar{\nabla} P + \frac{\bar{F}}{m} + \frac{\eta}{\rho} \nabla^2 \bar{u} + \frac{1}{3} \frac{\eta}{\rho} \nabla(\nabla \cdot \bar{u}) \tag{8}$$

where ρ is the density, $\bar{u}$ the velocity, P the pressure, η the viscosity, and $\bar{F}$ represents external forces such as Coulomb forces. The last two terms represent the viscous stress. In addition to these two equations we must satisfy the quasistatic Maxwell equations (or the corresponding gravitational equations)

$$\nabla \cdot \bar{E} = \frac{\rho}{\varepsilon} \tag{9}$$

$$\nabla \times \bar{E} = 0 \tag{10}$$

We assume here that proton currents in a nucleus produce second-order forces during the flow.

The above equations can be reduced to the simpler incompressible equations

$$\nabla \cdot \bar{u} = 0 \tag{11}$$

and

$$\left(\frac{\partial}{\partial t} + \bar{u}\cdot\bar{\nabla}\right)\bar{u} = \frac{-1}{\rho}\bar{\nabla P} + \frac{\bar{F}}{m} + \frac{\eta}{\rho}\nabla^2\bar{u} \tag{12}$$

for cases of low Mach number M, defined by

$$M = \frac{u}{s} = \frac{L}{sT} \tag{13}$$

where s is the speed of sound and L and T are a characteristic length and time. An expansion of equations (7) and (8) in terms of M^2 results in equations (11) and (12) to first order[16]. In the nuclear case, using $L = 5$ fm, $T \geq 10$ dsec, and $s \sim 5$ fm/dsec gives $M \leq 0.1$, so the incompressible approximation appears to be good. (An upper limit for the velocity of sound in weakly interacting Fermi liquids is given by $s = v_F/\sqrt{3}$, where v_F is the Fermi velocity[34].)

Analytical solutions to equations (11) and (12) are not generally available. Up to now calculations in nuclear physics have been carried out by assuming further that the viscosity is negligible and that the flow is irrotational ($\nabla \times u = 0$). In the last section we discussed the potential importance of viscosity in nuclear fusions. The assumption of irrotational flow is not valid for viscous drop dynamics, for reasons discussed below. Measurements of the energies of rotating nuclei indicate that the nuclear moment of inertia lies between a rigid-body value and an irrotational-flow value[17], although the moment of inertia approaches a more rigid value at high spins[35].

Taking the curl of equation (12) shows that the vorticity $\bar{\Omega} = \nabla \times \bar{u}$ obeys the diffusion equation

$$\frac{\partial\bar{\Omega}}{\partial t} = \bar{\nabla} \times (\bar{u} \times \bar{\Omega}) + \frac{\eta}{\rho}\nabla^2\bar{\Omega} + \bar{\nabla} \times \frac{\bar{F}}{m} \tag{14}$$

When $\Omega = 0$ (irrotational flow) and the external forces are conservative ($\nabla \times \bar{F} = 0$) then $\partial\Omega/\partial t = 0$; that is, irrotational motion is conserved in the bulk material if $\Omega = 0$ at any time. This is related to the Kelvin Circulation Theorem, which states that in the absence of viscosity the circulation $\Gamma = \oint \bar{u} \cdot d\bar{\ell} = \int_S \bar{\Omega} \cdot ds$ is strictly conserved. However, in cases involving the free surface of a viscous liquid, this result becomes invalid; that is, irrotational motion is not conserved even if $\Omega = 0$ at a certain time. This is because there is a delta-function velocity field at the free surface which creates a surface vorticity that is diffused inward via the term $\eta/\rho\ \nabla^2\bar{\Omega}$. Thus the degree of conservation of vorticity is given by the dimensionless Reynold's number $Re = \rho\ L\ U/\eta$, where L and U are a characteristic length and velocity. If $Re \gg 1$ then vorticity is conserved in the bulk because it diffuses only very slowly from the surface. However drops starting from rest can develop a bulk vorticity if the viscosity is high enough ($Re \ll 1$ or $\eta/\rho \gg 1/LU$). In the collision of viscous drops, the tangential viscous stress does not vanish at the point of contact and momentum is transferred over the

boundary, creating vorticity that leads to rotational motion. Thus the effect of nuclear viscosity on grazing collisions is to "drag" the colliding system around the center of mass. This fact has been noted recently by Wilczynski[18] and others[19,20,21] in relation to heavy ion experiments.

B. The Boundary Conditions at the Free Surface

By integrating the bulk equations (7) and (8) over the free surface we obtain the boundary conditions at the free surface. Physically these reflect the property that liquids can support no shear stress and that the normal stress at the surface defines the opposing fluid pressure at the surface. It can be shown[16] that the resultant stress on a free surface must vanish even though the surface is accelerating, for the surface has no inertia associated with it. The appropriate boundary condition becomes

$$\bar{n} \cdot (\overleftrightarrow{T}^{out} - \overleftrightarrow{T}^{in}) = 0 \tag{15}$$

where $\bar{n}$ is the normal to the surface and $\overleftrightarrow{T}$ is a general tensor whose divergence equals the right side of the Navier-Stokes equation. For a general charged or gravitating viscous drop the tensor $\overleftrightarrow{T}$ is composed of four separate tensors:

$$T_{ab} = P_{ab} + S_{ab} + V_{ab} + M_{ab} \tag{16}$$

where

$$P_{ab} = -\delta_{ab} P \quad \text{(normal fluid pressure)} \tag{17}$$

$$S_{ab} = \delta_{ab} \gamma \left(\frac{1}{R_1} + \frac{1}{R_2} \right) \quad \text{(surface tension)} \tag{18}$$

$$V_{ab} = \eta \left(\frac{\partial u_a}{\partial x_b} + \frac{\partial u_b}{\partial x_a} \right) \quad \text{(viscous stress)} \tag{19}$$

$$M_{ab} = \varepsilon \left(E_a E_b - \frac{1}{2} \delta_{ab} E^2 \right) \quad \text{(Maxwell stress)} \tag{20}$$

If the dielectric constant of nuclear matter is unity, that is, if nuclear matter is not polarizable, then the electric field is continuous over the surface and the Maxwell stress does not enter into the boundary condition (15). This will be assumed to be the case. However it is interesting to point out that if there is a tangential Maxwell stress on the surface it could result in convective and rotational flow in the interior of the drops during certain processes.

A salient characteristic of this problem is that the interesting dynamics enter through the surface boundary conditions. The bulk dynamics are preset by the surface pressure and the surface velocity through equations (11) and (12).

In general the combined bulk and surface equations are not analytically solvable, and one must resort to computer solutions by means of finite differences. One type of computer solution is described in the next subsection.

C. The Computer Code SQUISH

The recent advent of large and fast research computers has led to a widespread interest in hydrodynamic codes capable of solving the Navier-Stokes equation in two dimensions. Some codes have been written for compressible, high Reynolds number ($Re = \rho LU/\eta$) flow, and others for incompressible, low Re flow. Some use mainly Lagrangian techniques (particle-based coordinates) and others use Eulerian techniques (fixed coordinates). The type used for the work reported in this paper is the hybrid SMAC (Simplified Marker And Cell) method developed by Harlow and Amsden at Los Alamos for low Re flow[22]. (Typical nuclear flow has Re = 1). In this technique, which is illustrated in Figure 5, the drop is contained in a fixed Eulerian mesh and movable Lagrangian particles are injected into the cells of the mesh. A special set of surface markers keeps track of the free surface. Typical full and surface cells are shown in the insets of the figure. The forces and pressures are calculated at the centers of the cells, and velocities are deposited on the cell boundaries. The code first calculates a set of velocities over the cells by solving the bulk equations in finite-difference form. These velocities deposit the correct vorticity throughout the drop. Then it adjusts the velocities to conserve volume and to satisfy the boundary conditions in such a way that the vorticity remains correct. It does this by making all the velocity adjustments equal to the gradient of some quantity, so that the adjusting increment does not contribute to the curl of the velocity. This numerical method was proposed by Chorin[23]. After satisfying the volume conservation, vorticity requirements, and boundary conditions, a unique solution has been achieved, and the computer then moves the particles according to the local velocities for a small time step δt. The time is incremented, new forces are calculated, and the code proceeds in this cyclical manner to follow the dynamical paths of all the particles that make up the drop.

The advantages of this method are that it contains (a) a free surface that requires no parameterization, (b) a free-flow velocity field that can be rotational or irrotational, and (c) provisions for including any calculable external force, or any bulk property such as viscosity and elasticity. The limitations are that (a) the code is axially symmetric, (b) a reasonable mesh size has a finite error associated with it, and (c) the physics is purely classical, although some quantum mechanical properties can be simulated in a pseudo-classical manner such as adding a local elasticity.

The surface tension is calculated using the method developed by Foote[24] for meteorological studies. In this method a cubic spline is fitted to the free surface markers, and the local radii of curvature are calculated from the spline derivatives. The surface tension is applied as a pressure in the surface cells of the mesh. Coulomb forces have been calculated in a variety

of ways, the most accurate being the method used by Hill and Wheeler in their early attempts to simulate fission[25]. The method of Frankel and Metropolis has been used to calculate the Coulomb energy[26].

A more detailed account of the numerical methods used in SQUISH will be reserved for a paper dedicated to that purpose. In summary, the present version of SQUISH is capable of calculating the following properties of viscous charged liquid drops as a function of time: (a) free surface shape and energy, (b) free-flow velocity field (rotational or irrotational), (c) kinetic energy distribution, (d) center-of-mass kinetic energy, position, velocity, and moments, (e) Coulomb forces and energy, (f) free-flow moment of inertia, and (g) free-flow electric quadrupole moment. The accuracy of these calculated quantities depends on the size chosen for the finite-difference mesh. These quantities can also be studied as a function of viscosity and the initial shape and velocity field. In the next section we present some of these studies.

IV. SIMULATIONS OF DROP DYNAMICS

As an illustration of the versatility of such a code, let us examine the motion of a particular drop as we change its shape, viscosity, and charge. In the following figures the units are scaled to nuclear dimensions, but the non-nuclear scientist can scale them to his own field with the help of Table I. One entertaining byproduct of SQUISH is that it produces 16-mm films of the processes it simulates, and some of the figures in this paper represent smoothed composites of the motion picture sequences generated by the computer.

A. Oscillations

We begin with a study of the oscillations of an uncharged drop. In the limit of small amplitude and small viscosity ($\eta/\omega\rho R_0^2 \ll 1$), the free surface as a function of time is given by Lord Rayleigh's expression[27]

$$R = R_0 \left(1 + \Sigma\, A_n\, e^{-\beta t} \cos(\omega t) P_n(\theta)\right) \tag{21}$$

where

$$\beta = (n-1)(2n+1)\,\frac{\eta}{\rho R_0^2} \tag{22}$$

with characteristic frequency

$$\omega^2 = n\,(n-1)\,(n+2)\,\frac{\gamma}{\rho R_0^3} \tag{23}$$

where γ is the surface tension coefficient and R_0 is the radius of the equivalent sphere. In all the following drop simulations, γ has been given the nuclear value of 1 MeV/fm^2. For uranium nuclei the period of the undamped oscillation is about 16 dsec.

Wong and Tang[28] have discussed the analytical solutions to small amplitude oscillations of charged and uncharged drops in terms of complex Bessel functions. We shall now study large-amplitude oscillations, for which there is no analytical theory. The sequence shown in Figure 6 simulates the oscillations of a drop with an initial shape given by the second-order Legendre polynomial, with the coefficient $a_2 = 0.4$. The viscosity in all these figures is given as the kinematic viscosity $\nu = \eta/\rho$. In figure 6 ν is of a medium value that results in damped oscillatory motion. The drop is started at rest; then the initial excess surface energy (SE) is exchanged in time for kinetic energy (KE) as the drop oscillates from a prolate spheroid (maximum SE and minimum KE) to a sphere (maximum KE and minimum SE) and then through an oblate spheroid and a sphere to a prolate spheroid at the end of one period. The drop simulations at the top of the figure are from the film strip; the large dots are the free surface markers and the smaller interior dots are the cell particles. There are about a thousand particles in this drop. The internal patterns in these simulations are produced by ghost images in the camera and do not necessarily represent real flow patterns. The total energy of this oscillating drop is seen to decrease exponentially as the damping proceeds. The period of oscillation, 15.4 dsec, is slightly longer than the theoretical Rayleigh period for small-amplitude oscillations, which is 13.4 dsec. The viscous damping factor is given within the accuracy of the code by the Rayleigh value $\beta = 0.088$. The Rayleigh equation still describes the general behavior quite satisfactorily, even though the ratio of oscillation amplitude to drop radius is not very small. This result has been observed experimentally by fluid mechanicians many times.

The simulation in Figure 7 shows this same drop except that the viscosity has been increased by a factor of ten. Now the motion is overdamped and the drop slowly damps out to a sphere with no oscillatory behavior. The viscous damping factor yielded by this run is $\beta = 0.17$, while the corresponding Rayleigh factor is $\beta = 0.88$. The Rayleigh theory, of course, does not apply to this overdamped, large-amplitude case.

In Figure 8 the size of the drop has been changed so that it now has an initial Legendre coefficient given by $a_2 = 1.0$. This very large-amplitude motion is nonlinear and does not preserve the P_2 shape. In the least square fit of the free surface shown on the left, a substantial a_4 component is seen to grow with the motion, and this is also very evident in the simulated drop sequences at the top of the figure. The energy changes are shown on the right; at the end of this simulation there is a sphere with a great deal of kinetic energy which will probably proceed into some complex oblate spheroidal shape, still following the general Rayleigh behavior. The extrapolated period from this initial quarter-cycle simulation is about twice the corresponding Rayleigh period. Recently Prosperetti has studied the initial-value problem for small-amplitude oscillations[29], and has found that a drop that is initially critically damped in the Lamb theory[30] should have an aperiodic decay for short times and a damped oscillatory motion at later times, and the initial damping is higher than the value used by Wong and Tang[28]. The frequency predicated by normal-mode analysis is only true at later times. More studies of this early-time effect will be made by carrying out these simulations for several periods.

The addition of a full body charge to the drop involves a substantial increase in computer running time as well as some loss in accuracy. In Figure 9 are shown the smoothed energy curves for the same drop that we have discussed previously in Figure 6 except that it now has a volume charge of 62 proton charges. The charge density, like the mass density, is assumed to be constant throughout the drop, in agreement with our observation of constant nuclear charge densities. This particular charge represents a ^{152}Sm nucleus, which is known to be stable against fission even for fairly large distortions. In this simulation the surface forces still predominate the motion, but now the surface energy is exchanged for Coulomb energy as well as kinetic energy, resulting in a longer period for the oscillation than is exhibited for the corresponding uncharged drop. The Coulomb energy and the kinetic energy are at a maximum for the spherical shape. The extension to gravitating drops merely involves changing the sign of the Coulomb interaction and replacing $1/4\pi\varepsilon_0$ with the gravitational constant G, and the charge density by the corresponding mass density. Toward the end of this simulation, the motion has damped out to small-amplitude oscillations about a sphere. The accuracy of these calculations is about one percent.

In the next subsection we discuss the behavior of this drop as more charge is added to it until it fissions.

B. Fissions

In Figure 10 is plotted the kinetic energy of the drop after a fixed time interval as a function of the atomic charge Z of the drop. For small charges the motion is oscillatory. As the charge is increased, the Coulomb forces oppose the surface tension more strongly, slowing down the motion until the two forces just balance at the minimum in the curve. This minimum represents a saddle point between oscillation and fission; for charge densities beyond this point the Coulomb forces predominate and the drop begins to fission with no oscillatory behavior. The saddle point charge predicted by SQUISH in this curve is in good agreement with the theoretical saddle point charge of 79 predicted for this shape by Cohen and Swiatecki[31]. In Figure 11 is shown the same drop of Figure 10 with charge Z = 110. Here the Coulomb energy plunges down as the fission proceeds, and the surface energy and kinetic energy move up almost equally in the initial stages of the motion.

The dimensionless parameter that is used to represent the relative strengths of the Coulomb force and the surface tension is the fissility, defined by

$$x = \frac{1}{2}\frac{E_{coul}}{E_{surf}} . \qquad (24)$$

This parameter was first introduced in the celebrated paper of Bohr and Wheeler[32] in which the liquid drop model of nuclear fission was successfully used to account for many observed fission data.

In Figure 12 is shown a comparison of two simulations of a drop that was initialized with a shape corresponding to an x = 0.9 saddle shape, but with enough charge to make x = 1.56. This highly charged drop is expected to fission very rapidly. The drop at the top of the figure was given a high viscosity that would lead to overdamped oscillations at lower charge densities, and the drop at the bottom was given a lower viscosity that would lead to damped oscillations such as in Figure 6. The central time scale applies to both drop sequences. The effect of the increased viscosity is most noticeable in the longer time scale of the more viscous process, but otherwise the shape development seems to be about the same for the two cases. This highly charged drop does not pinch off quickly into two fragments, but rather becomes very elongated, developing a long thin neck that apparently will not pinch off until the neck has extended to virtually no width.

Such a thin neck should not be described by macroscopic hydrodynamics, since its width is less than the mean free path of the individual nucleons. In this case a microscopic approach is appropriate, and such a treatment is probably necessary to explain the asymmetric mass distribution observed for fission fragments from heavy nuclides. It is possible that microscopic fluctuations cause a pinch-off at some time during the development of this long thin neck, and if the fluctuations are randomly distributed along the neck then the fragment mass distribution would be naturally asymmetric.

The details of the velocity field in the lower viscosity drop are shown in Figure 13. The z-component of velocity is shown above the drop profile as a function of the cylindrical coordinates r and z. The value of v_z is averaged over the disks shown in the profile. The variation of v_z with r, which is shown for the shaded disk, is constant to one percent, implying that the Werner-Wheeler ρ-independent transport method[33] used by Nix is indeed applicable to fission studies of drops started at rest with small viscosities. The average vorticity of the shaded disk is 0.02 $dsec^{-1}$, so the corresponding rotational period is of the order of 600 dsec. Since this period is much longer than the fission process time, the vorticity is negligible. This is expected from the Kelvin circulation theorem discussed earlier, which states as a corollary that a drop starting at rest under conservative forces must preserve zero vorticity in its subsequent motion if the viscosity is small (Re >> 1). The vorticity is more appreciable in the higher-viscosity fission, as can be seen from the internal structure in Figure 12.

The pre-scission development of the center-of-mass velocity of the fission fragments is shown in Figure 14 as a function of time. For comparison, the solid line in the figure represents the velocity development of two spherical fragments initially tangent and at rest. The limiting velocity for these two spheres is 2.14 fm/dsec. It is difficult to extrapolate the limiting velocity for an x = 1.56 nucleus from the experimental values, which extend only up to x = 0.92, but a rough extrapolation yields a limiting velocity of around 2.5 fm/dsec. It appears from this preliminary simulation that the lower-viscosity fissions will yield the experimental value for v_∞ more closely than the higher viscosity fissions, which will result in too low a limiting velocity. Further tests of this nature are in progress that will allow a direct comparison with experiment. These tests might yield a definite upper limit for the

nuclear viscosity during fission. This apparent low viscosity during fission reinforces our concept of nuclear fission as a low-temperature and therefore low-viscosity process. The effects of viscosity in nuclear fission probably can be expected to be much smaller than in nuclear fusion.

C. Fusions

The problem of the fusion of two colliding liquid drops is a difficult numerical problem because of the high distortion in the initial stages of contact. Our fusion results are still preliminary and the details will be reserved for a subsequent paper. However we show in Figure 15 a simulation representing the head-on collision of two ^{152}Sm nuclei at rather high velocities. The Weber number for this collision is around 5.5, so surface tension effects should be negligible compared to inertial effects. The general features of this viscous fusion are that the necking process involves a large amount of viscous friction which hinders the formation of the neck and hence the fusion. If the two drops cannot fuse together to a stable saddle shape, the composite drop will begin to fission immediately. The implication of this for the fusion of heavy nuclei is quite serious, if nuclear viscosity is indeed high at these excitation energies, for it implies that at high accelerator velocities the viscosity may hinder the formation of compound nuclei, while at low velocities the Coulomb repulsion makes complete fusion impossible. Therefore there may be only a narrow range of energies for which compound nucleus experiments can be performed in the heavy nuclei. We are exploring this question in more depth at the present time.

V. SUMMARY

We have presented a brief survey of the oscillations, fissions, and fusions of classical viscous liquid drops scaled to nuclear dimensions. In the first part of this paper we have taken some care to describe under what conditions the nuclear fluid can be expected to approximate a classical macroscopic drop. This approximation is necessary because of the complexity of solving the corresponding quantum mechanical equations for several hundred highly excited nucleons.

We have included a nuclear viscosity in our studies because it can apparently explain some of the data recently accumulated in heavy ion accelerator experiments, notably the unexpected difficulty in fusing two heavier nuclei into a stable compound system. However other explanations may be possible, and the nuclear viscosity may yet prove to be negligible for all the processes we have considered. It is hoped that future experiments that carefully study the cross section for complete fusion as a function of energy will resolve this question once and for all.

The results presented here and in forthcoming papers have applications in many diverse fields that involve the interaction and motion of classical drops. Among them are meteorology, space science, aerosol technology, astrophysics, and of course fluid dynamics. Although this particular paper has been written primarily for the nuclear scientist, we plan to present future studies in a dimensionless manner that makes them accessible to all these fields.

REFERENCES

1. Lord Rayleigh, "On the Capillary Phenomena of Jets", Proc. Roy. Soc. (London) 29, 71, (1879).

2. S. Chandrasekhar, "The Oscillations of a Viscous Liquid Globe" Proc. London Math. Soc. (3) 9, 141, (1959).

3. W. H. Reid, "The Oscillations of a Viscous Liquid Drop", Quart. Appl. Math. 18, 86, (1960).

4. H. H. K. Tang and C. Y. Wong, "Vibration of a Viscous Liquid Sphere" submitted to J. Physics A.

5. A. J. Sierk and J. R. Nix, "Dynamics of Fission and Fusion with Applications to the Formation of Superheavy Nuclei", Los Alamos Scientific Laboratory Report LA-UR-73-931, (August, 1973).

6. R. W. Hasse, "Dynamic Model of Asymmetric Fission", Nuc. Phys. A128, 609, (1969).

7. K. A. Brueckner, "Many-Body Problem for Strongly Interacting Particles. II. Linked Cluster Expansion", Phys. Rev. 100, 36, (1955).

8. J. D. Bernal, "The Structure of Liquids", Sci. Am. 203, 124, (1960).

9. M. Reiner, "Rheology", in Handbook of Physics, E. U. Condon and H. Odishaw, eds., McGraw-Hill, New York, 3-40, (1958).

10. W. D. Myers and W. J. Swiatecki, "Nuclear Masses and Deformations", Nuc. Phys. 81, 1, (1956).

11. J. C. Wheatley, "Experimental Properties of Liquid ^{3}He at Very Low Temperatures", Quantum Fluids, North-Holland, Amsterdam, 183, (1966).
also
R. T. Johnson, D. N. Paulson, C. B. Pierce, and J. C. Wheatley, "Measurements Along the Melting Curve of ^{3}He at Millikelvin Temperatures" Phys. Rev. Lett. 30, 207, (1973).
also
R. A. Webb, T. J. Greytak, R. T. Johnson, and J. C. Wheatley, "Observation of a Second-Order Phase Transition and Its Associated P-T* Phase Diagram in Liquid ^{3}He", Phys. Rev. Lett. 30, 207, (1973).

12. G. N. Flerov and U. T. Oganesyan, "Nuclear Reactions Induced by Xenon Ions and Experiments on Synthesizing Superheavy Elements", Dubna, P7-6523 (1972); translation by C. T. Alonso available from the author.
also,
I. Zvara, "Studies of the Heaviest Elements at Dubna", Dubna, E12-7547, (1973).

13. R. Wieczorek, R. W. Hasse, and G. Sussman, "First Estimates of the Nuclear Viscosity Constant from the Damping of the Fission Dynamics", Paper IAEA-SM-174/02, Third International Symposium on the Physics and Chemistry of Fission, Rochester, N.Y., 13-17 August, (1973).

14. T. A. Alvesalo, Yu. D. Anufriyev, H. K. Collan, O. V. Lounasma, and P. Wennerstrom, "Evidence for Superfluidity in the Newly Found Phase of ^{3}He" Phys. Rev. Lett. 30, 962, (1973).

15. K. A. Brueckner, "The Present Status of the Theory of Nuclear Structure", Many Body Theory, Ryogo Kubo, ed., Syokabo, Tokyo and Benjamin, New York, (1966).

16. J. R. Melcher, Field-Coupled Surface Waves, M.I.T. Press, Cambridge, Massachusetts, (1963).

17. K. Alder, A. Bohr, T. Huus, B. Mottelson, and A. Winther, "Study of Nuclear Structure by Electromagnetic Excitation with Accelerated Ions", Rev. Mod. Phys. 28, 432, (1956).

18. J. Wilczynski, "Nuclear Molecules and Nuclear Friction", Phys. Lett. 47B, 484, (1973).

19. C. F. Tsang, "Nuclear Collisions With Friction", LBL-2928, Nobel Symposium on Superheavy Elements, Ronaby, Sweden, June 10-14, (1974). To be published in Physica Scripta.

20. R. H. Davis, "Dissipative Capture in Heavy Ion Fusion", preprint.

21. J. Bondorf, "Theory of Highly Inelastic Transfer Processes", International Conference on Reactions Between Complex Nuclei, Nashville, Tennessee, June 10-14, (1974).

22. A. A. Amsden and F. H. Harlow, "The SMAC Method: A Numerical Technique for Calculating Incompressible Fluid Flows", LASL-LA-4370, (1970).

23. A. J. Chorin, "Numerical Solution of the Navier-Stokes Equations", Math. Comp. 22, 745, (1968).

24. G. B. Foote, "A Numerical Method for Studying Liquid Drop Behavior", J. Comp. Phys. 11, 507, (1973).

25. D. L. Hill and J. A. Wheeler, "Nuclear Constitution and the Interpretation of Fission Phenomena", Phys. Rev. 89, 1102, (1953).

26. S. Frankel and N. Metropolis, "Calculations in the Liquid-Drop Model of Fission", Phys. Rev. 72, 914, (1947).

27. H. Lamb, Hydrodynamics, Dover Publications, New York, 6th edition, 642, (1879).

28. H. H. K. Tsang and C. Y. Wong, "Vibration of a Viscous Liquid Sphere", submitted to J. Physics A.

29. A. Prosperetti, "On the Oscillations of Drops and Bubbles in Viscous Liquids", Paper IV-5, International Colloquium on Drops and Bubbles, Pasadena, California, 28-30 August, (1974).

30. H. Lamb, loc. cit., 642.

31. S. Cohen and W. J. Swiatecki, "The Deformation Energy of a Charged Drop; Part V", Annals of Physics 22, 406, (1963).

32. N. Bohr and J. A. Wheeler, "The Mechanism of Fission", Phys. Rev. 56, 426, (1939).

33. J. R. Nix, "Further Studies in the Liquid-Drop Theory of Nuclear Fission", Nuc. Phys. A130, 241, (1969).

34. D. Pines and P. Nozieres, The Theory of Quantum Liquids, Vol. I (Fermi Liquids), Benjamin, New York, (1966).

35. R. A. Sorensen, "Nuclear Moment of Inertia at High Spin", Rev. Mod. Phys. 45, 353, (1973).

Table I. Unit Conversion Table

Quantity	Nuclear Unit		SI Unit
Time	1 dsec	=	10^{-22} sec
Length	1 fm	=	10^{-15} m
Mass	1 amu	=	1.66043×10^{-27} Kgm
Energy*	1 Mev	=	1.602×10^{-13} j
Velocity	1 fm/dsec	=	10^{7} m/sec
Kinematic viscosity**	1 fm^2/dsec	=	10^{-8} m^2/sec
Surface tension***	1 Mev/fm^2	=	1.602×10^{17} nt/m
Charge	1 e	=	1.6021×10^{-19} coul

* In terms of the fundamental units 1 amu $fm^2/dsec^2$ = 1.036 Mev

** The nuclear density is 0.13 amu/fm^3 = 1.66×10^{18} Kg/m^3. Thus a nuclear kinematic viscosity of 1 fm^2/dsec means a viscosity of 1.66×10^8 poise.

*** The nuclear surface tension is approximately 1 Mev/fm^2.

Some Numbers in Nuclear Units

c	=	velocity of light	= 30 fm/dsec
$\hbar$	=	Planck's constant/2π	= 6.353 amu fm^2/dsec
$4\pi\varepsilon_o$	=	Coulomb force constant	= 0.7196 e^2 $dsec^2$/amu fm^3
ρ	=	nuclear density	= 0.13 amu/fm^3
v_p	=	typical nucleon velocity in the nucleus	$\approx$ 8 fm/dsec
f_n	=	nuclear force at 1.5 fm	$\approx$ 15 amu fm/$dsec^2$
f_{pp}	=	p-p Coulomb force at 1 fm	= 1.39 amu fm/$dsec^2$
R_o	=	radius of uranium sphere	= 7.57 fm

FIGURE CAPTIONS

Figure 1 (a) Radial distribution function f_r as a function of distance r from a particle center r_o in idealized gases, liquids, and solids.

(b) Nearest-neighbor correlation strength c_n as a function of time t at a particle center r_o in gases, viscoelastic liquids, and solids. The parameter λ is the relaxation time for stresses in a viscoelastic liquid.

Figure 2 (a) Measured temperature dependence of the viscosity of the Fermi liquid ^{3}He [11]. The effect of the small pairing correlation is to lower the curve to the left of the minimum.

(b) Speculation of the temperature dependence of the viscosity of nuclear matter. The strong pairing correlation could force the viscosity to zero at very low temperatures.

Figure 3 Representation of how heavy ion experiments fit into the transition from the quantum mechanical to the classical regimes. The internal energy of an ideal Fermi gas is given by

$$U = \frac{3}{5} N \epsilon_F \left(1 + \frac{5}{12}\pi^2 \left(\frac{kT}{\epsilon_F}\right)^2\right)$$

where ϵ_F is the Fermi energy (typically 40 Mev for nuclei). Thus the quantum mechanical excitation energy is approximately $E^* = \frac{A}{4} \frac{(\pi kT)^2}{\epsilon_F}$ for nuclear Fermi gases. The excitation of classical gases is given by $E^* = \frac{3}{2} A(kT)$. The transition point is taken at the temperature where the de Broglie wavelength $\lambda\!\!\!^{-}$, given by $\lambda\!\!\!^{-} = \frac{\hbar}{p} = \sqrt{\frac{\hbar^2}{2MkT}}$, equals the internucleon spacing d, which is around 1.5 fm. Beyond about 100 Mev of excitation energy the nuclear matter is no longer incompressible and the internucleon spacing should increase with temperature. Bulk heavy ion phenomena such as fission and fusion lie in the transition region between $\lambda\!\!\!^{-} = 5d$ and $\lambda\!\!\!^{-} = d/5$.

Figure 4 A schematic comparison of the properties of nuclear matter with two other Fermi liquids, ^{3}He and the electron gas.

Figure 5 A schematic description of how the two-dimensional code SQUISH solves the finite-difference equations for fluid flow while satisfying the boundary conditions at the free surface of a viscous incompressible fluid.

Figure 6 Surface oscillations of a viscous uncharged drop as a function of time. Details are described in the text.

Figure 7 Overdamped motion of a viscous uncharged drop as a function of time. This drop is identical to the drop in Figure 6 except that the viscosity is ten times higher here.

Figure 8 Nonlinear oscillation of a viscous uncharged drop as a function of time. This drop has the same viscosity as the drop in Figure 6, but the amplitude of its distortion from the sphere is greater. The Legendre coefficients are obtained from a least square fit to the free surface.

Figure 9 Surface oscillations of a charged viscous drop as a function of time. This drop is the same as the drop in Figure 6 except that it has a body charge of 62 proton charges, making it a classical ^{152}Sm liquid drop.

Figure 10 The total kinetic energy of the drop of Figure 9 at time t = 4 dsec, plotted as a function of the drop charge Z. The minimum lies on the three-dimensional saddle point that separates fission behavior from oscillatory behavior.

Figure 11 The drop of Figure 9 with Z = 110. This drop lies on the fission side of the saddle point, so it begins to separate immediately. Such a highly charged drop does not exist in nature.

Figure 12 Comparison of two descents from saddle toward scission for a mythical nucleus with Z = 160 and A = 300. The viscosity of the drop at the top is ten times higher than the viscosity of the drop at the bottom. Both drops were started from rest, so the flow is irrotational.

Figure 13 Details of the velocity field calculated by SQUISH for the lower drop in Figure 12. The flow is irrotational (negligible vorticity) and the variation of v_z with r constant.

Figure 14 Center-of-mass velocities of the pre-scission fragments of the two drops in Figure 12. The higher viscosity drop will have a lower fragment velocity at scission. For comparison, the solid curve follows the center-of-mass velocity of two initially tangent spheres whose total volume equals the drop volume. From studies such as these we can estimate how the limiting velocity at infinity depends on viscosity.

Figure 15 Head-on collision of two classical ^{152}Sm drops.

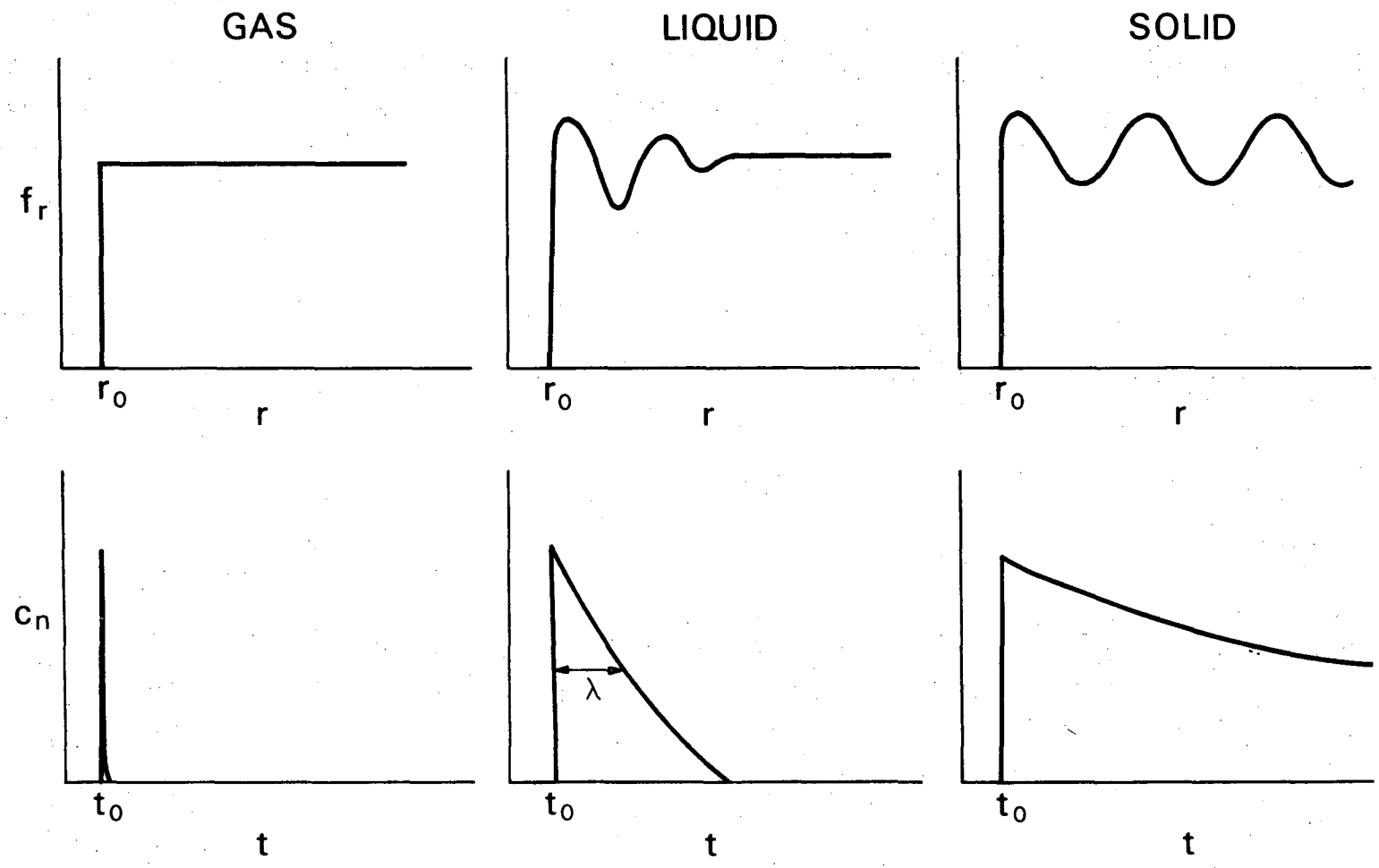

Figure 1

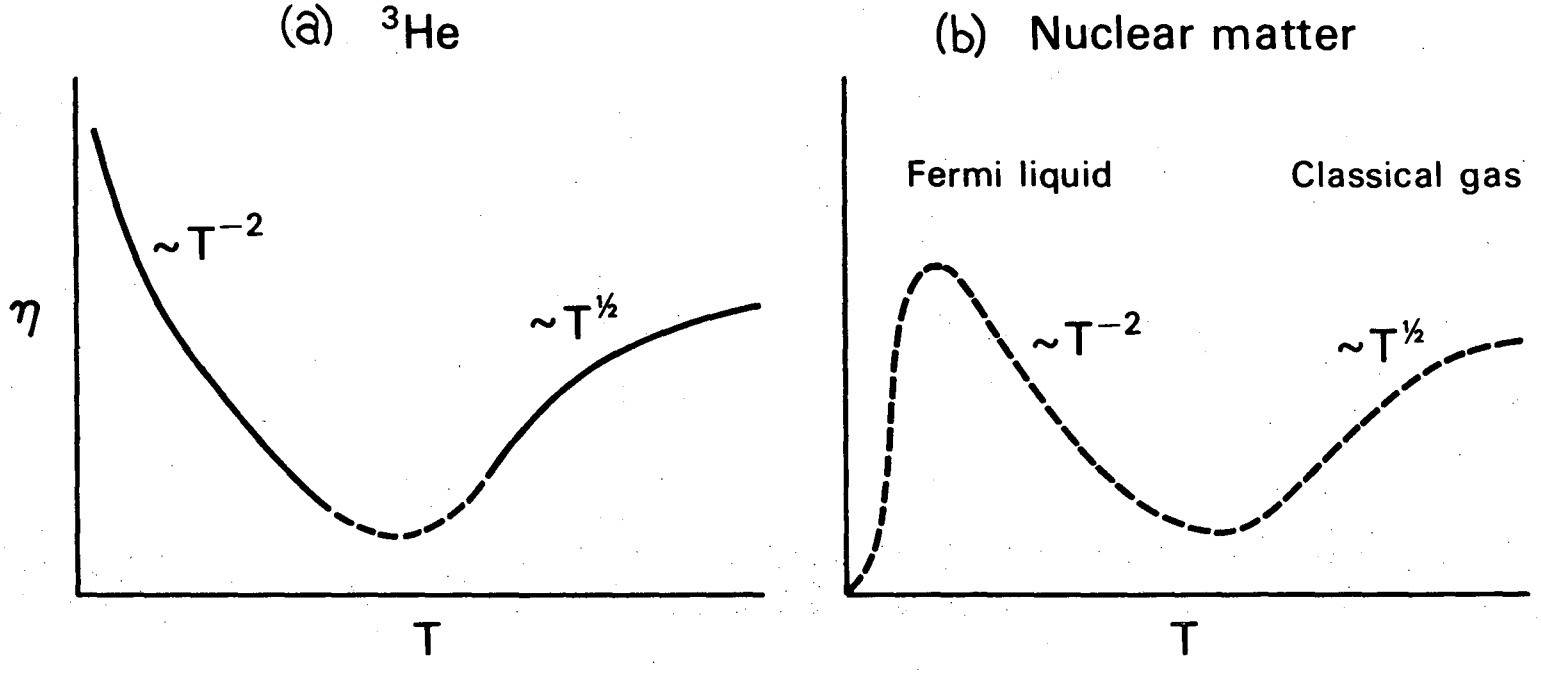

XBL 749-4939

Figure 2

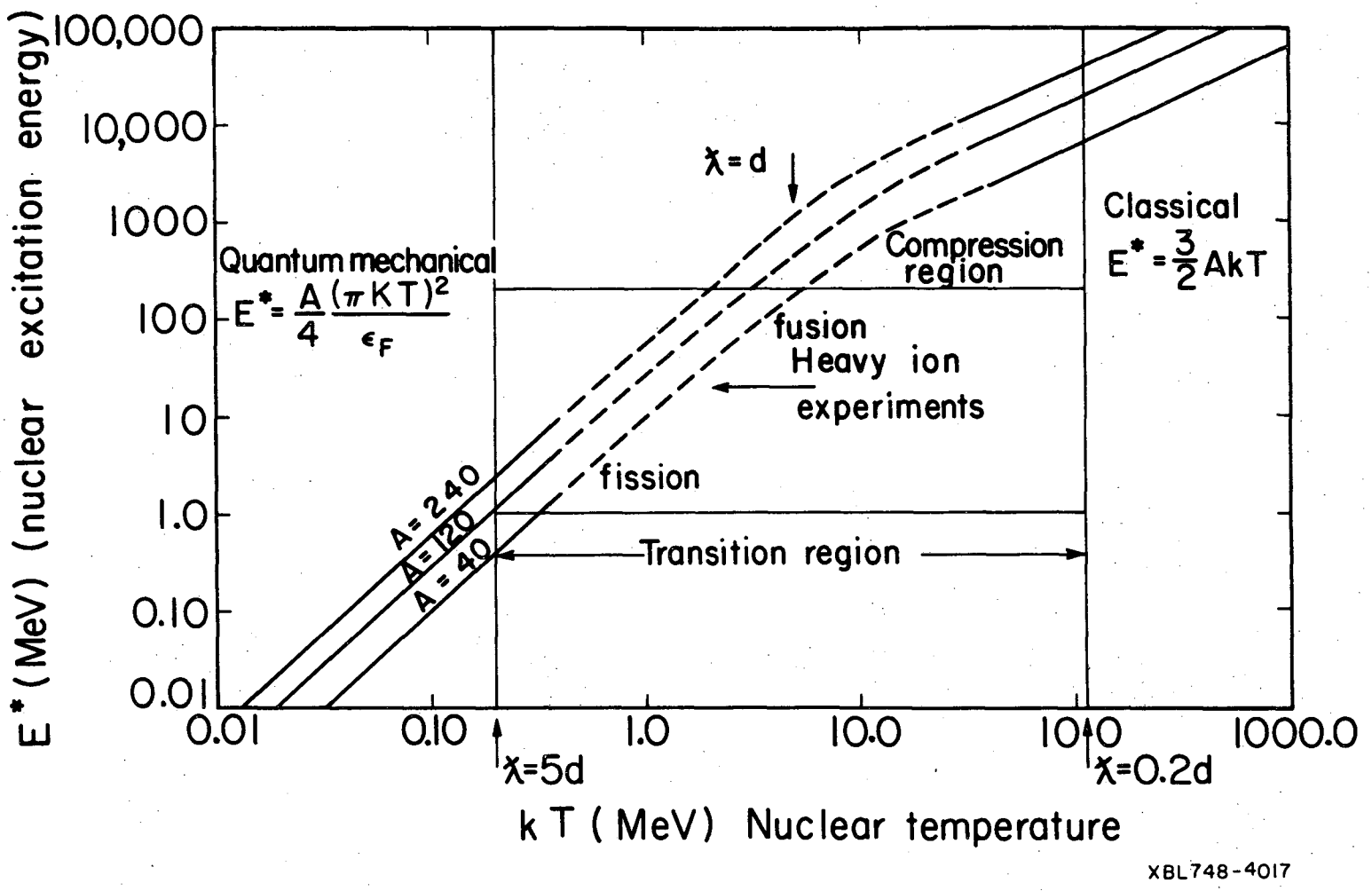
E* (MeV) (nuclear excitation energy)
100,000
10,000
1000
100
10
1.0
0.10
0.01
Quantum mechanical
$E^* = \frac{A}{4}\frac{(\pi KT)^2}{\epsilon_F}$
ƛ = d
Compression region
Classical
$E^* = \frac{3}{2}AkT$
fusion
Heavy ion
experiments
fission
A = 240
A = 120
A = 40
Transition region
0.01
0.10
1.0
10.0
100
1000.0
ƛ=5d
ƛ=0.2d
k T (MeV) Nuclear temperature
XBL748-4017

Figure 3

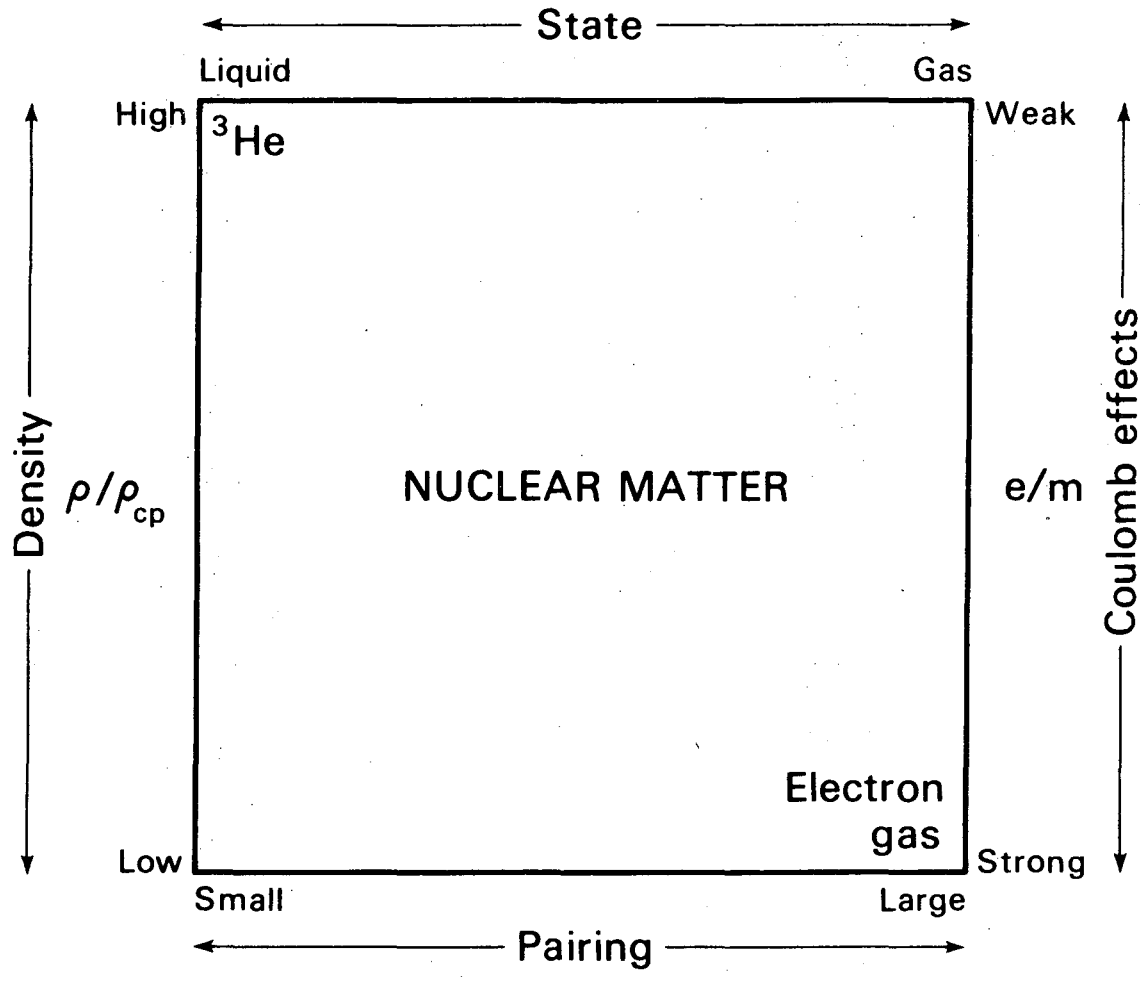

XBL 749-4940

Figure 4

SQUISH-HOW IT WORKS

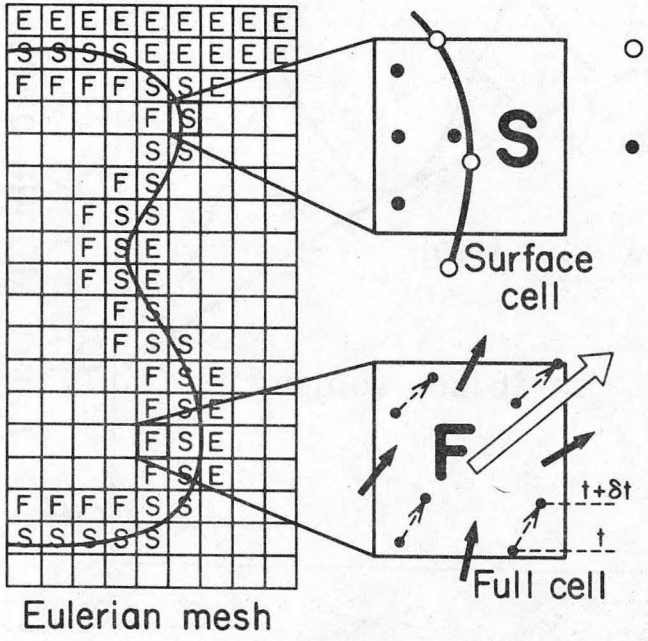

○ = Free surface marker

• = Lagrangian particle

Velocities stored on cell boundaries

Resultant force applied at cell center

1. Forces calculated from free-flow shape (surface tension and coulomb forces)
2. Velocities calculated from Navier-Stokes equation
$$\left(\frac{\delta}{\delta t}+\bar{u}\cdot\bar{\nabla}\right)\bar{u}=-\frac{1}{\rho}\,\bar{\nabla}P+\frac{\bar{F}}{m}+\frac{n}{\rho}\,\nabla^2\bar{u}$$
3. Volume conserved from incompressibility $\bar{\nabla}\cdot\bar{u}=0$
4. Move cell particles and surface markers and advance time to $t+\delta t$

The SMAC method (Harlow and Amsden, Los Alamos)

XBL748-4016

Figure 5

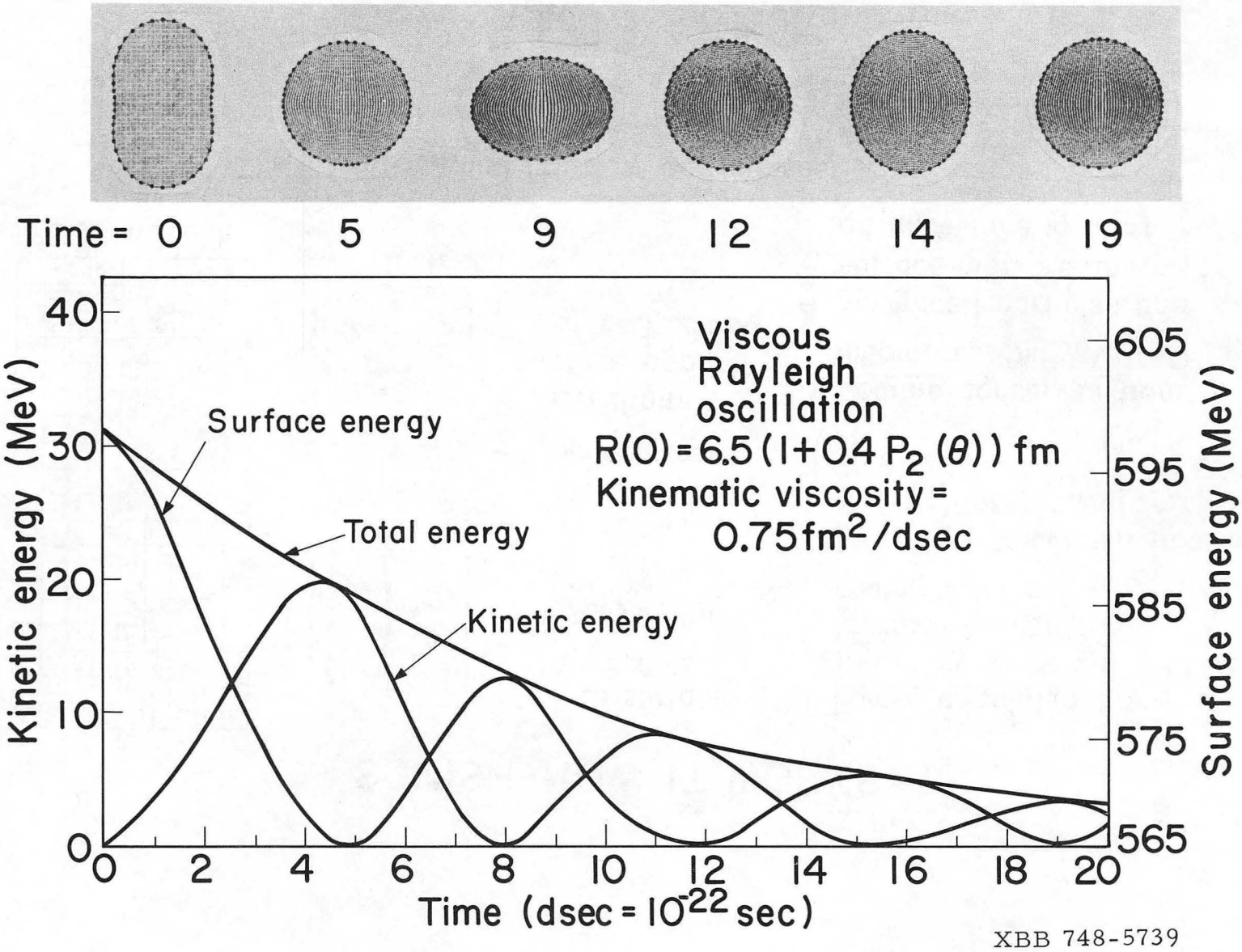
Time = 0
5
9
12
14
19
Viscous
Rayleigh
oscillation
R(0) = 6.5 (1 + 0.4 P2 (θ)) fm
Kinematic viscosity =
0.75 fm2/dsec
Surface energy
Total energy
Kinetic energy
Kinetic energy (MeV)
Surface energy (MeV)
Time (dsec = 10-22 sec)
0
10
20
30
40
565
575
585
595
605
0
2
4
6
8
10
12
14
16
18
20
XBB 748-5739

Figure 6

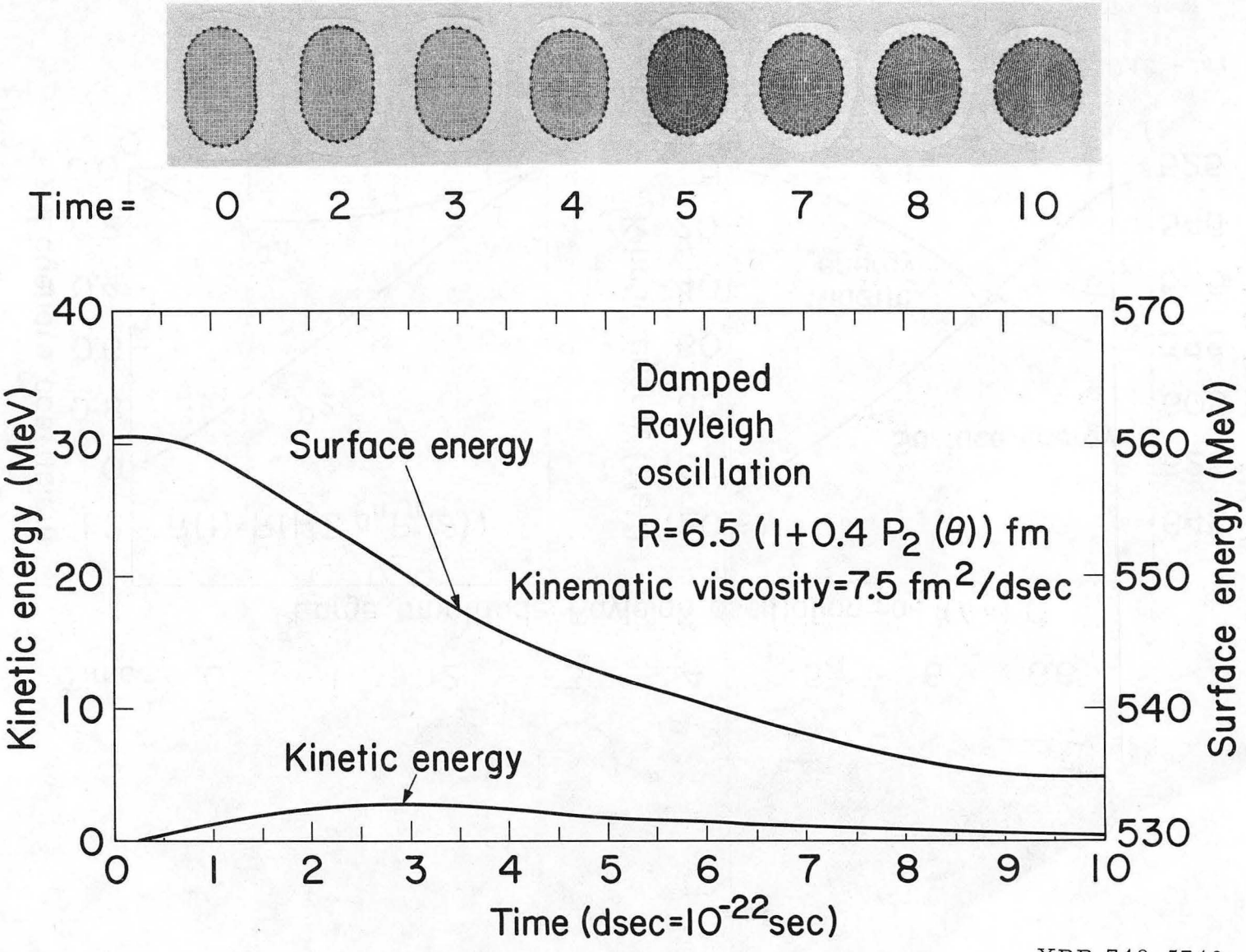

XBB 748-5740

Figure 7

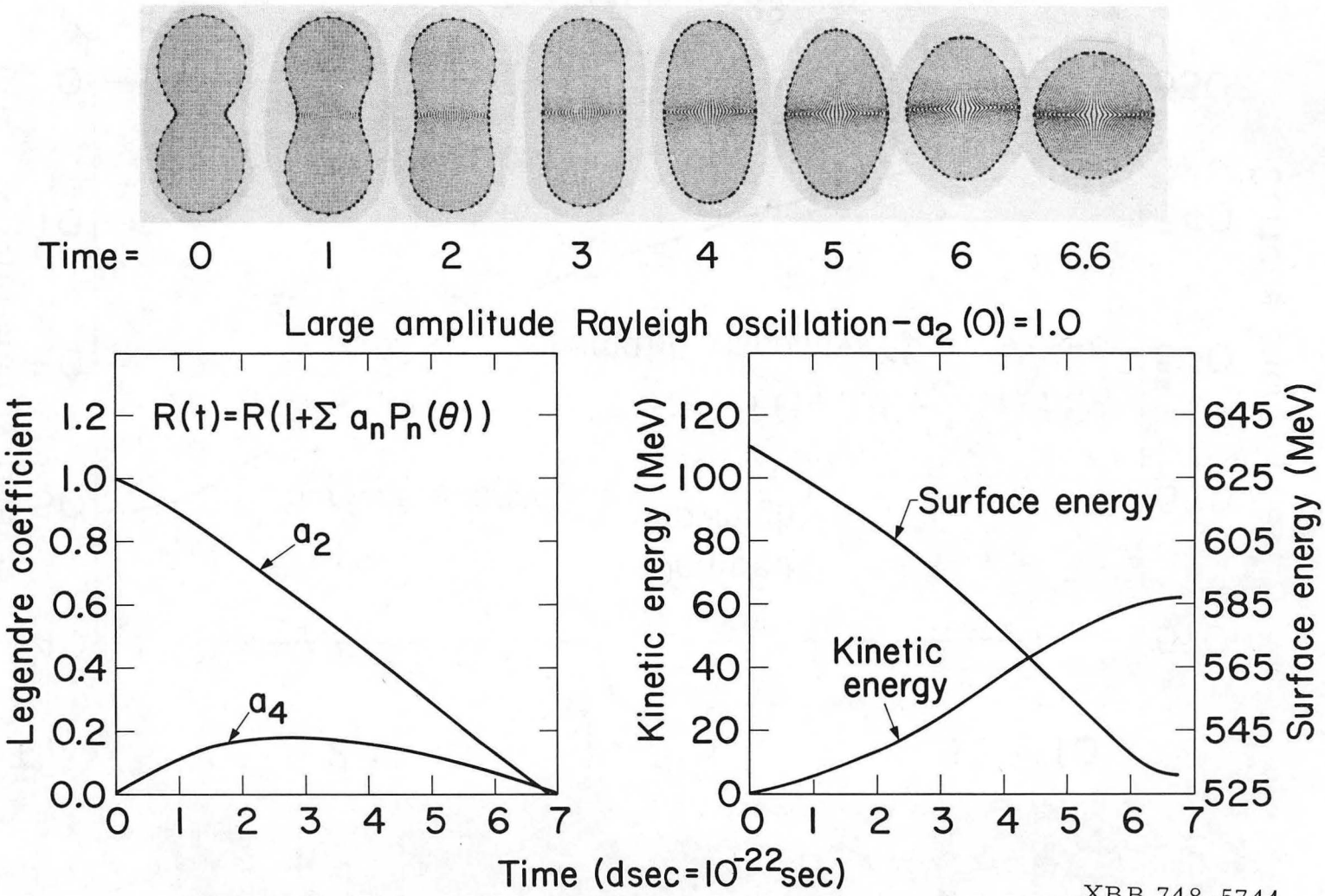

XBB 748-5741

Figure 8

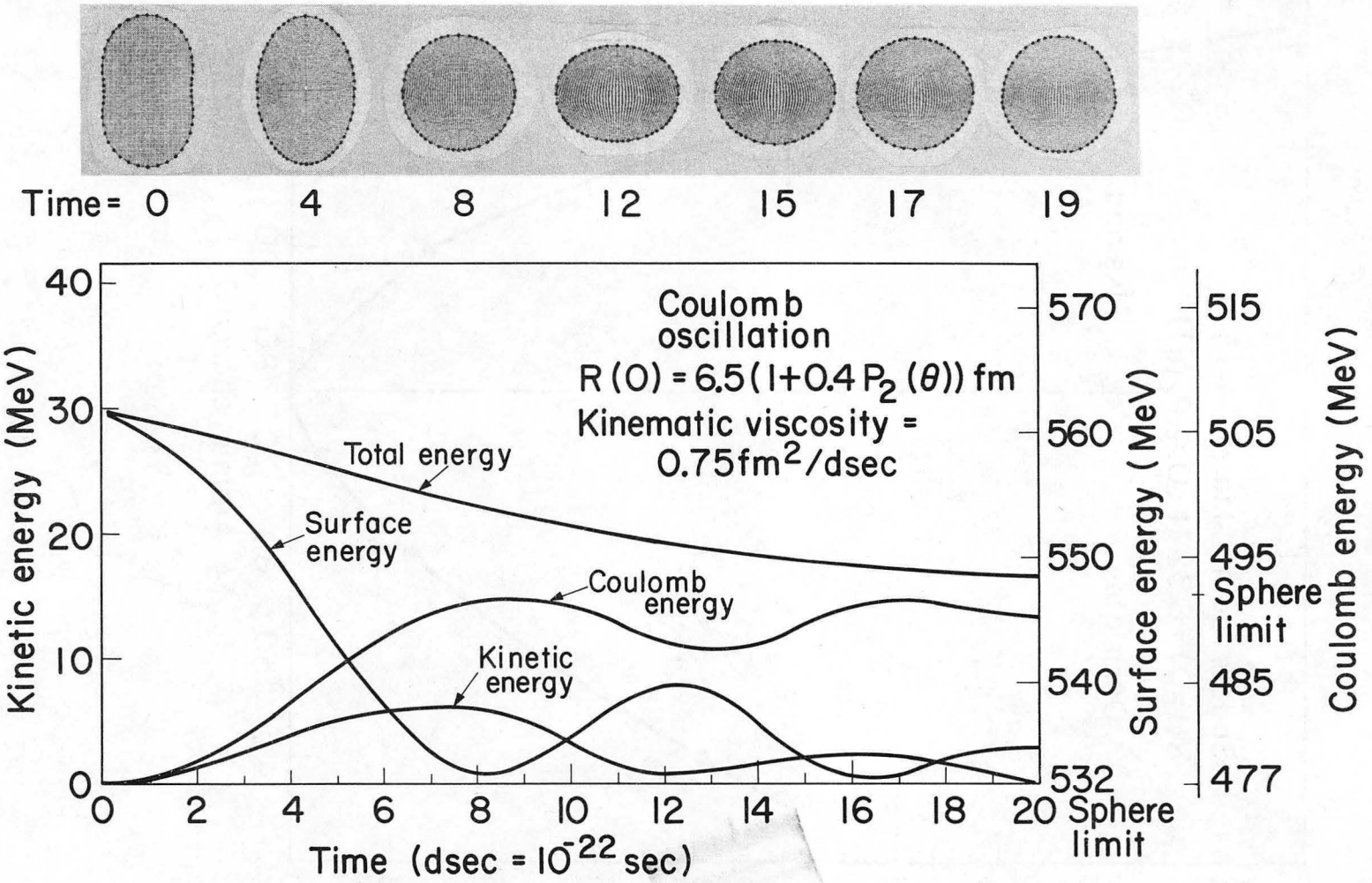

Figure 9

XBB 748-5738

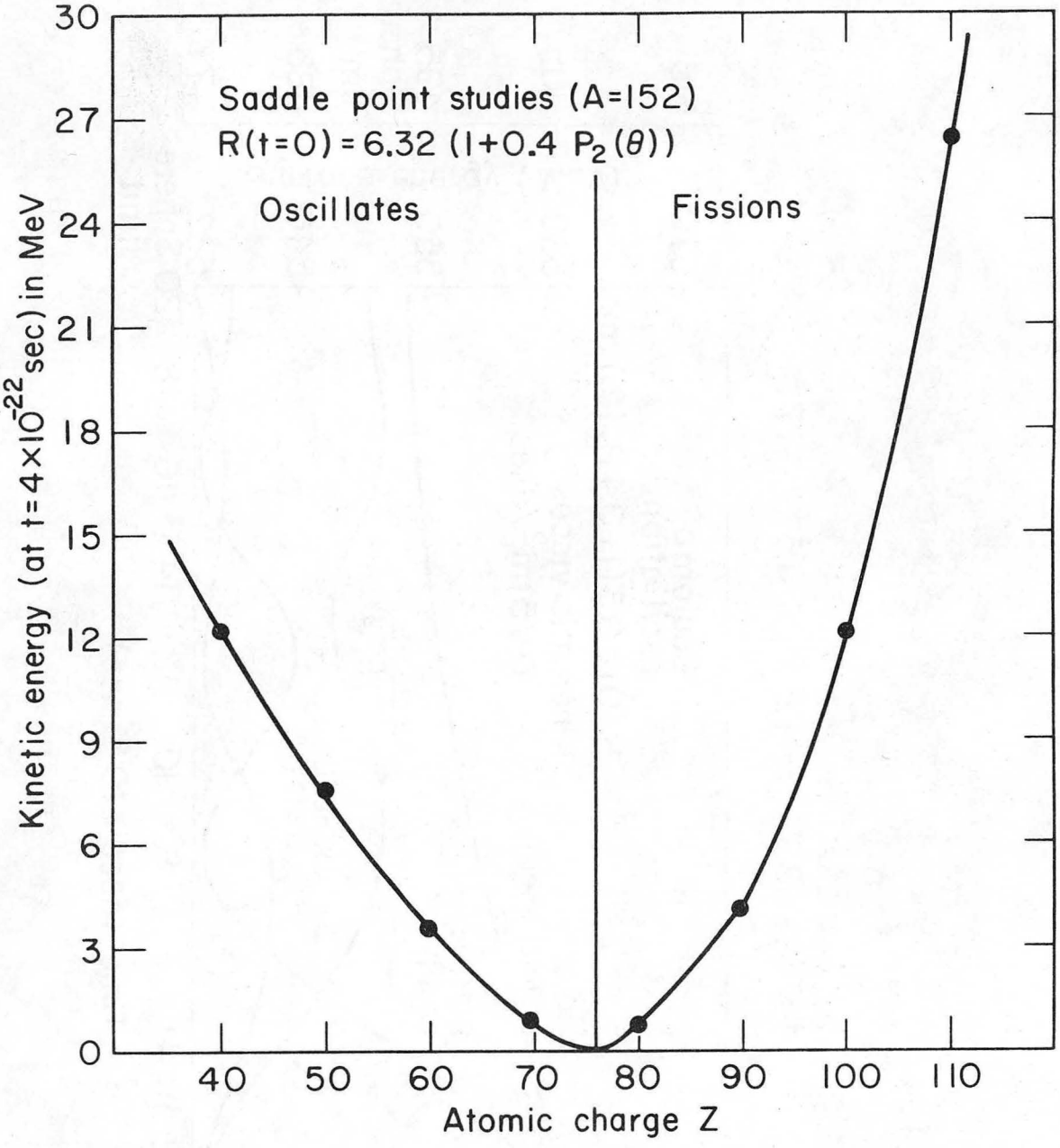

XBL 748-4018

Figure 10

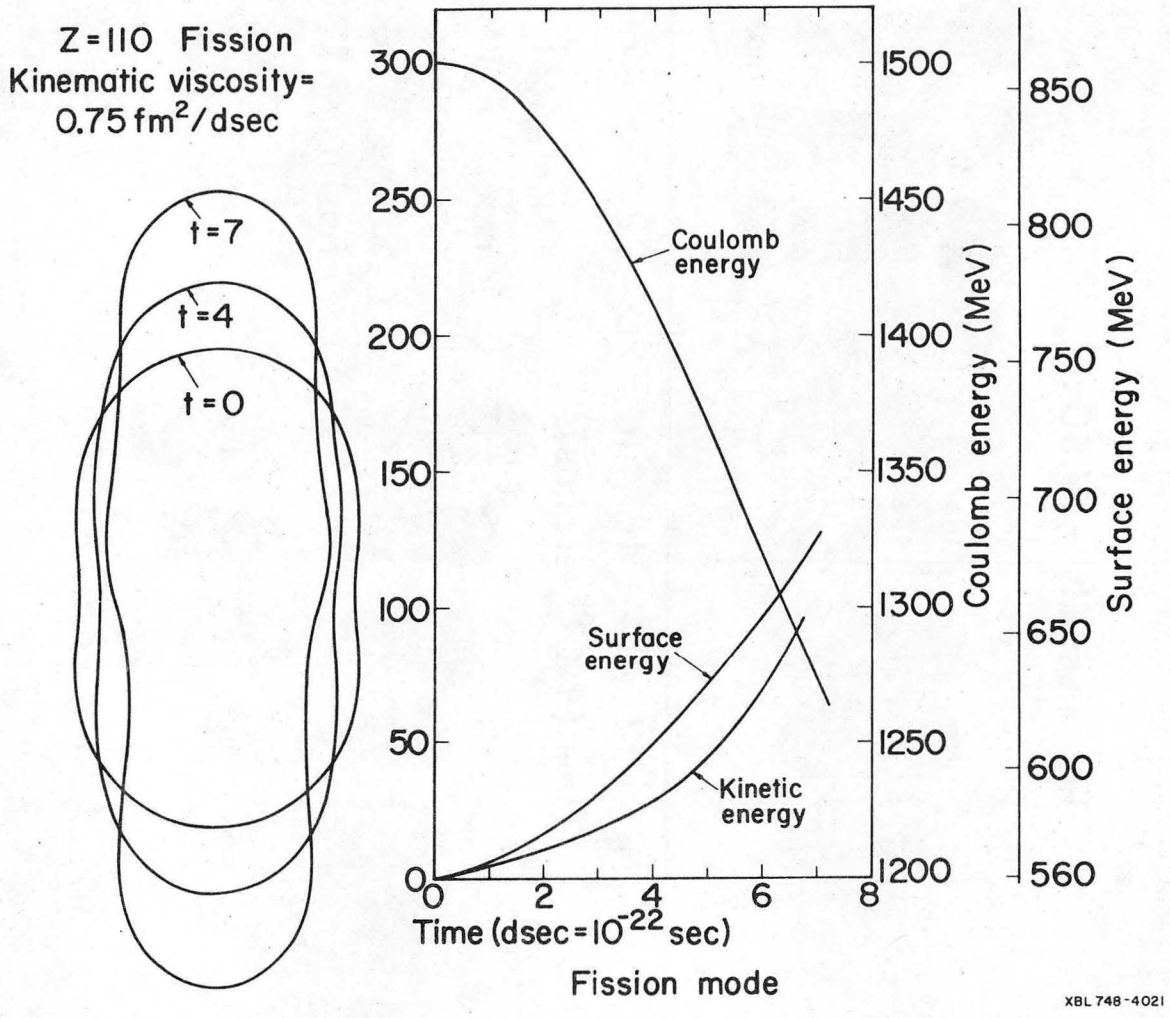
Z=110 Fission
Kinematic viscosity=
0.75 fm²/dsec
t=7
t=4
t=0
Coulomb energy
Surface energy
Kinetic energy
Time (dsec=10⁻²² sec)
Fission mode
Coulomb energy (MeV)
Surface energy (MeV)
300
250
200
150
100
50
0
1500
1450
1400
1350
1300
1250
1200
850
800
750
700
650
600
560
0
2
4
6
8
XBL 748-4021

Figure 11

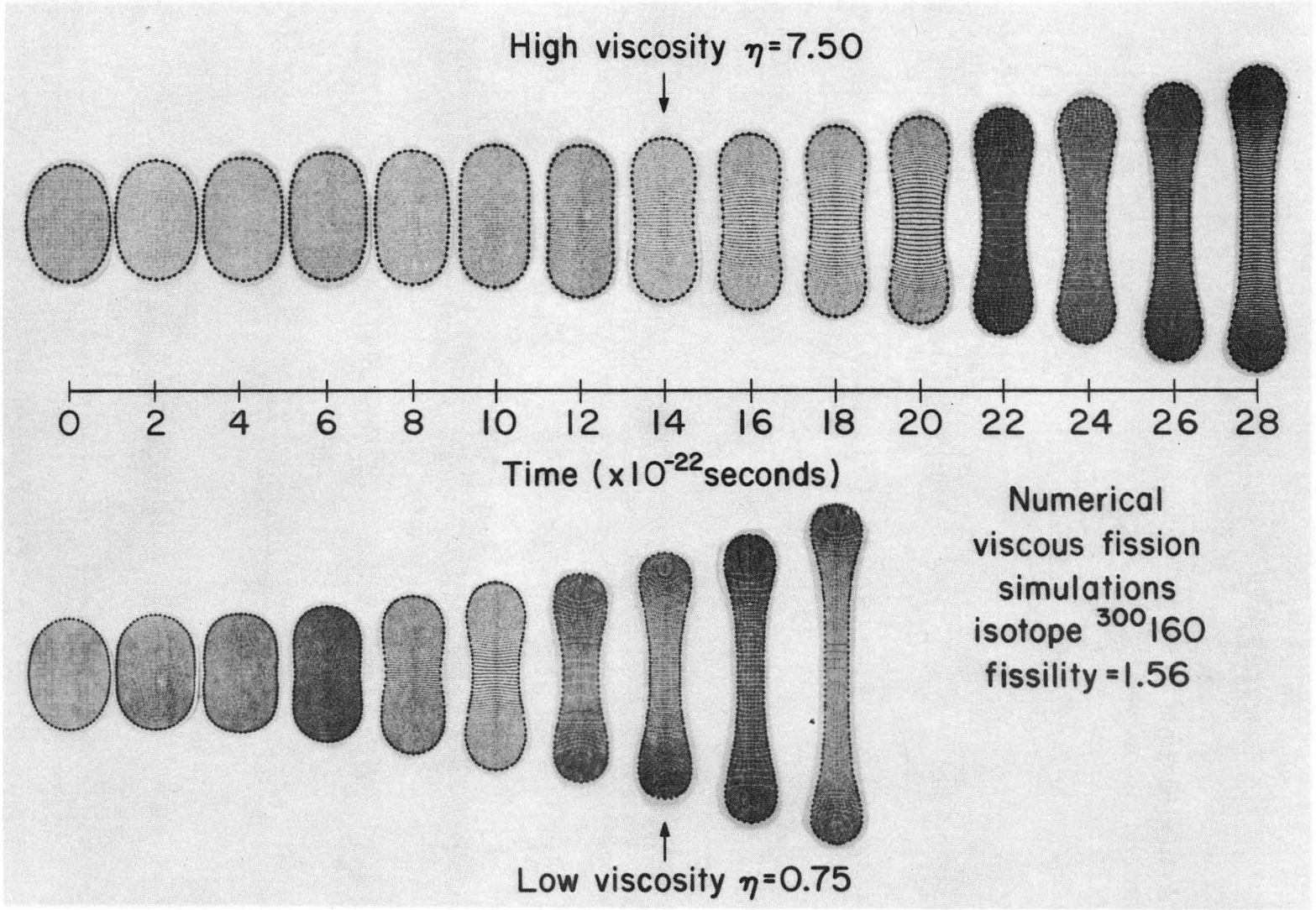

XBB 749-5975

Figure 12

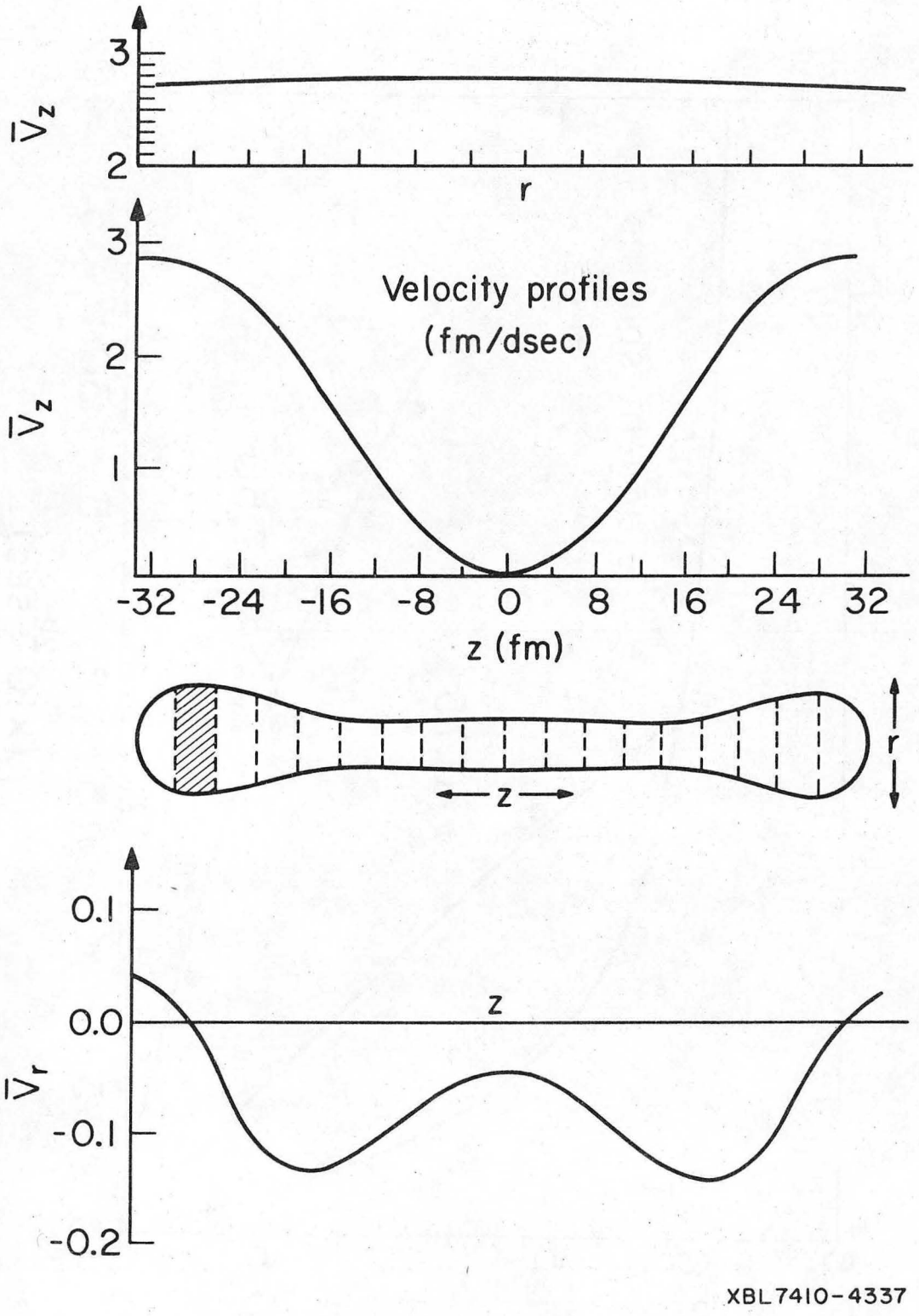
3
2
$\bar{V}_z$
r
3
2
1
$\bar{V}_z$
Velocity profiles
(fm/dsec)
-32 -24 -16 -8 0 8 16 24 32
z (fm)
r
z
0.1
0.0
-0.1
-0.2
$\bar{V}_r$
z
XBL7410-4337

Figure 13

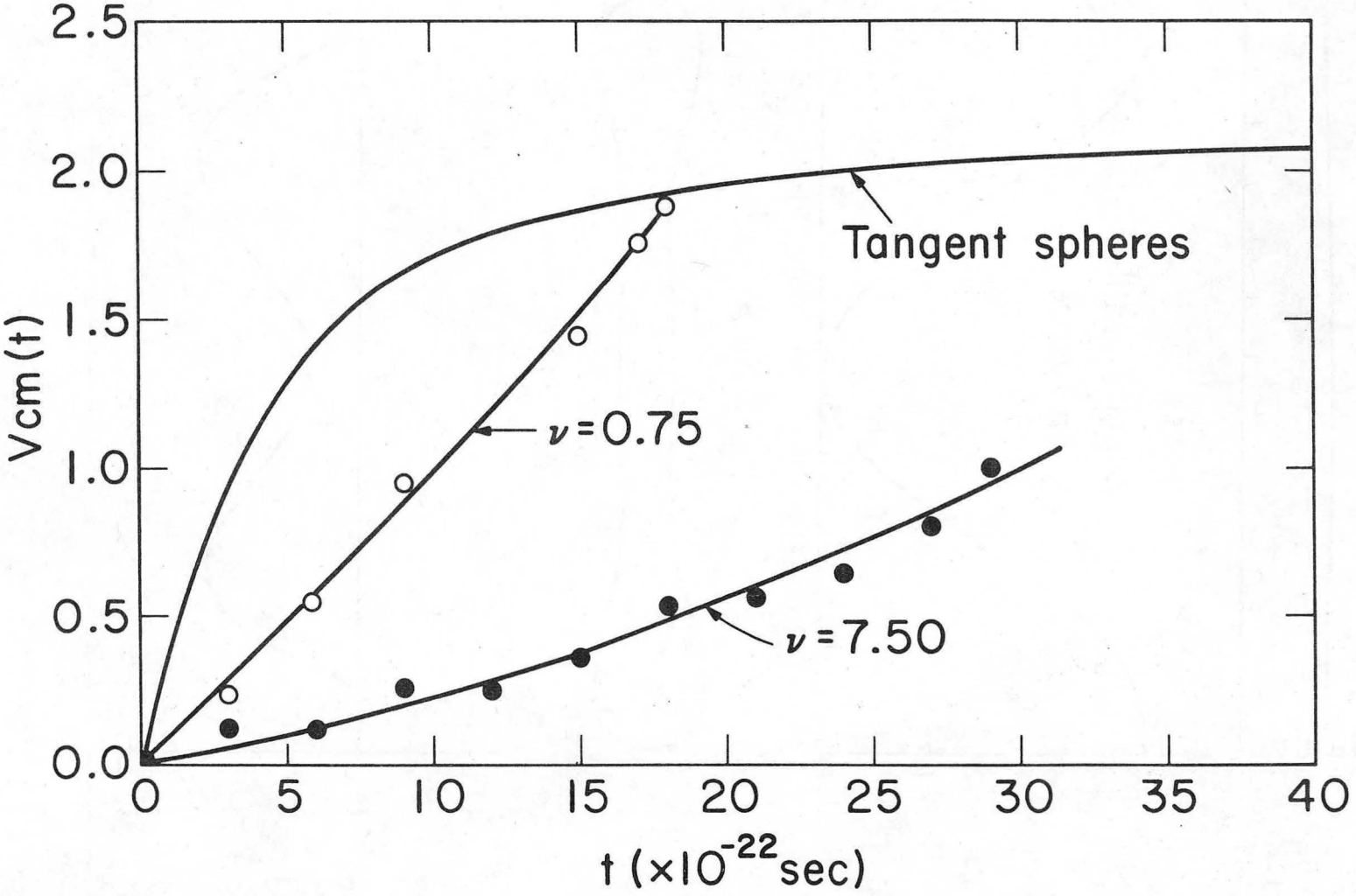

XBL 7410-4336

Figure 14

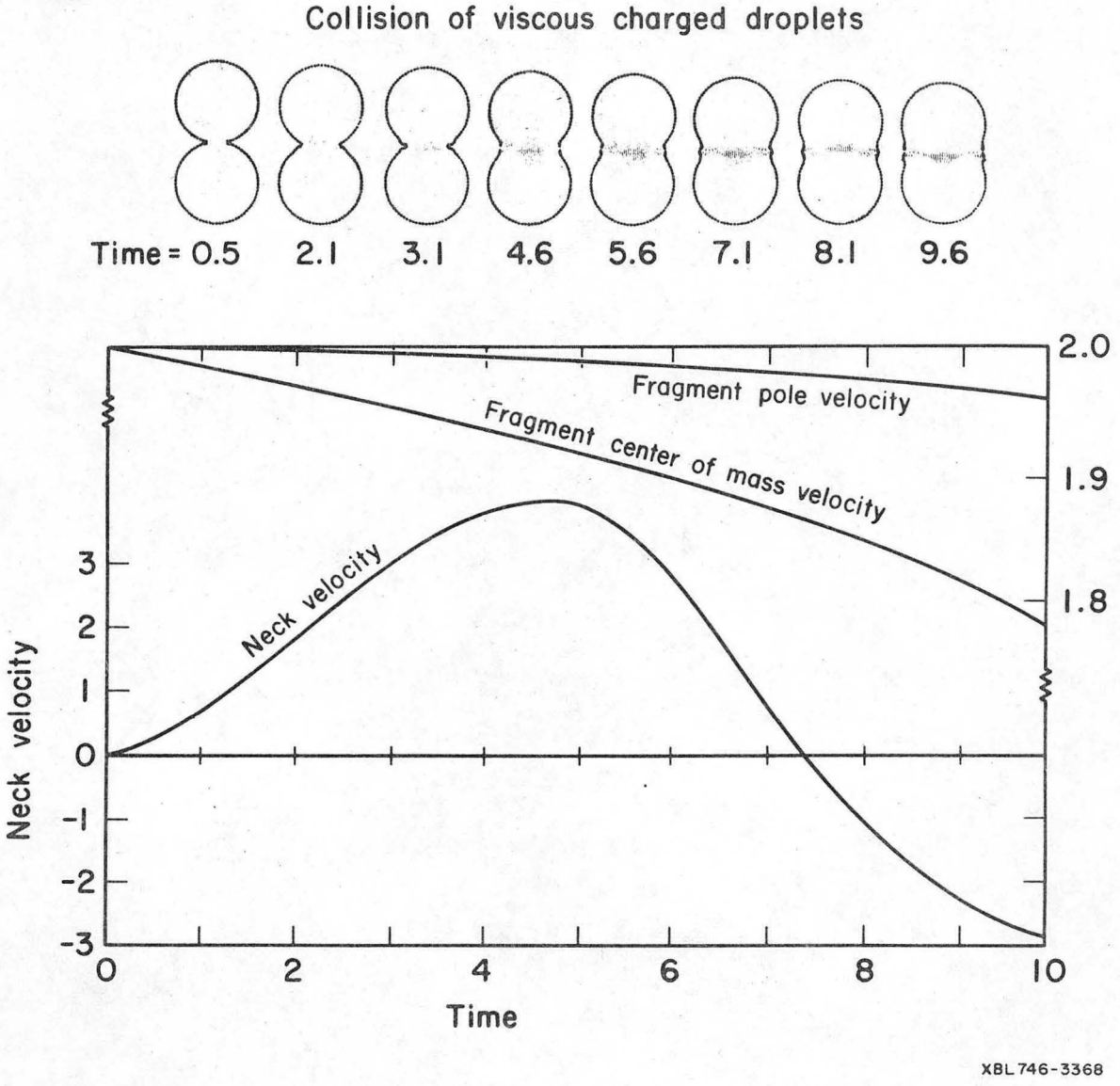
Collision of viscous charged droplets
Time = 0.5
2.1
3.1
4.6
5.6
7.1
8.1
9.6
Fragment pole velocity
Fragment center of mass velocity
Neck velocity
Neck velocity
Time
2.0
1.9
1.8
3
2
1
0
-1
-2
-3
0
2
4
6
8
10
XBL746-3368

Figure 15

TECHNICAL INFORMATION DIVISION
LAWRENCE BERKELEY LABORATORY
UNIVERSITY OF CALIFORNIA
BERKELEY, CALIFORNIA 94720